# Influence of UV and $\gamma$ radiation on optical features of YAG crystals doped with Ce, Pr, Nd, Ho, Tm, Cr and Mg

**Sławomir Kaczmarek[1], Andrej Matkowski[2], Zygmunt Mierczyk[1], Krzysztof Kopczyński[1], Dymitr Sugak[2], Zygmunt Frukacz[3]**

[1] Institute of Optoelectronics, Military University of Technology, Warsaw, Poland
[2] Institute of Materials, Lviv, Ukraine
[3] Institute of Electronic Materials Technology, Warsaw, Poland

## 1. Introduction

Crystals of yttrium-aluminium garnet doped with elements: Nd, Er, Ho and Pr are often applied in steady-state lasers emitting in the range of $0.6 \div 3$ mm. Sensibilization, i.e. doping these crystals with Ce, Cr and Tm ions is used for increasing their efficiency ofarc lamp pumping. These ions take up the greatest part of pump radiation and transfer it to generating ions. The sensibilization decreases the generation threshold and increases efficiency and radiation power. This method is essentially important for broad-band excitation with an arc lamp, when there are weak absorption bands in active, lasing ions for. Another method that improves laser characteristics of different crystals is their annealing at high temperatures (near melting point). During annealing process a partial removal of growth defects (e.g. oxygen vacancies) takes place. This method is a time-consuming one and requres special temperature program for annealing and slow cooling processes. The last investigations carried out for Er:YAG and CTH:YAG crystals [1] enable us to create, may be, the new method to improve the usefulness of crystals in laser applications: their excitation with $\gamma$ quanta of 1.25 MeV energy from $^{60}$Co source of radiation.

UV radiation emitted by pump xenon lamp generates nonstable colour centers in laser rods, what causes the instability of laser generation parameters (threshold or output energy). To avoid these effects, cut-off filters: 350 nm (sodium glass) or 450 nm (GG-5 filter) are applied in lasers.

Nonstable colour centers originate from the growth defects activated by UV radiation (oxygen and aluminium vacancies for garnet crystals). The same defects can be utilized for formation of stable colour centers in laser rods with exposure of $\gamma$ radiation. It makes sense for crystals with their AA bands placed within the range of their pumping bands. These bands overlap the pumping bands and increase efficiency of pumping processes and thus improve generation characteristics of these crystals.

Passing through the medium, $\gamma$ quanta lose energy as a result of: photoelectric absorption, Compton scattering and electron-positron pair creation. In all these processes there are produced electrons of energies comparable to energies of incident quanta. For photons of energies equal to about 1 MeV the dominant effect is Compton scattering [2]. During this process photon knocks out a reverse electron, losing part of its energy and changing its direction of motion.

Energy of ionizing radiation absorbed by medium divides between electron and ion subsystems of the crystal. The energy is absorbed mainly as a result of interaction between radiation particles and medium electrons. Only part of the energy is transferred to ions during collisions with primary or secondary electrons. The energy transferred to the ion subsystem increases temperature of the medium and creates radiation defects, so called Frenkle pairs, i.e., ions dislocated into intersitial sites and vacancies. To built a Frenkle pair it is necessary to perform the condition: $T > T_d$, where $T$ is energy taken by atom during collision with radiation particle, $T_d$ is energy threshold necessary for creating a singledefect (several eV up to 100 eV). Such mechanism is called "over-threshold collision mechanism" [2].

Energy transferred to electron subsystem excites it and ionizes the medium. Excitation of the electron subsystem produces Roentgen and optical excitons (plasmons), while ionization produces free carriers. Decomposition of electron excitations andrecombination of carriers can proceed in two ways: radiant and radiationless. In the last case the emitted energy can, in particular conditions, built a displacement defect. Displacement defects can also occur as a result of electrostatic repulsion between multiple ionized atoms of medium and their environment.

Ionizing radiation can create not only new structural defects but it also can rebuild (overcharge) and even partly "cure" existing growth defects. In particular it rebuilds and overcharges defect centers (Frenkle pairs). Series of measurements of absorption coefficient before and after UV and $\gamma$ excitations have been taken in order to determine the influence of ionizing radiation on YAG crystals features.

## 2. Results of spectroscopic investigations

Crystals were grown by Czochralski method from Ir crucibles in $N_2$ atmosphere in the Institute of Electronic Materials Technology (ITME).

Samples of YAG doped with Nd (1 at.%), Ce (0.05 at.%), both Ce and Nd (0.05 at.%, 1 at.%), Cr:Tm:Ho (0.36 at.% Ho, 5.7 at.% Tm, 1 at.% Cr), Er (33at.%), Pr (1 at.%), Cr in Mg,Cr:YAG – 0.003 at.%, with diameters of 10 mm and thickness of $1 \div 2$ mm, and both sides optically polished, were cut out from the most homogeneous parts of crystals and examined with Mach-Zehnder interferometer.

The samples have been excited with 10 pulses of UV radiation emitted by pumping xenon arc lamp. Pulse energy was equal to 42.2 J (115 J in the case of Er:YAG) and there was time interval

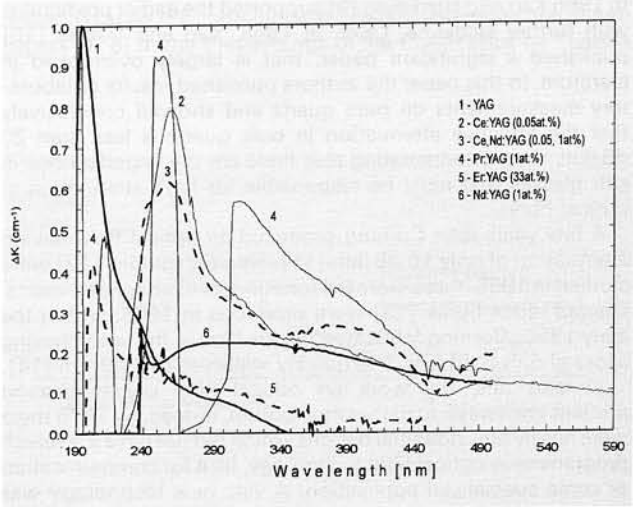


Fig. 1. Additional absorption bands for YAG crystal doped with Pr, Er, Nd, Ce, both Ce and Nd after UV excitation of xenon arc lamp

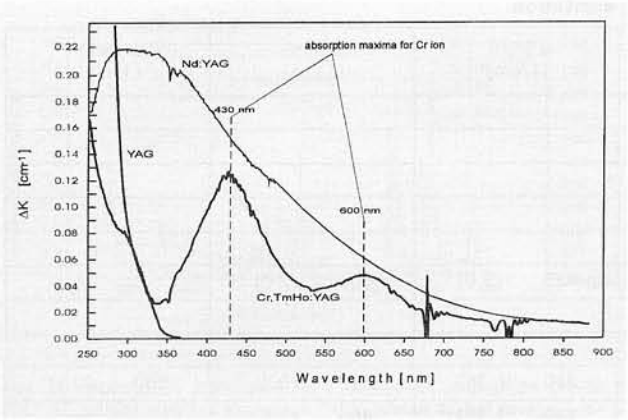


Fig. 2. Additional absorption bands for YAG crystal doped with Cr, Tm, Ho and Nd after UV excitation with xenon arc lamp

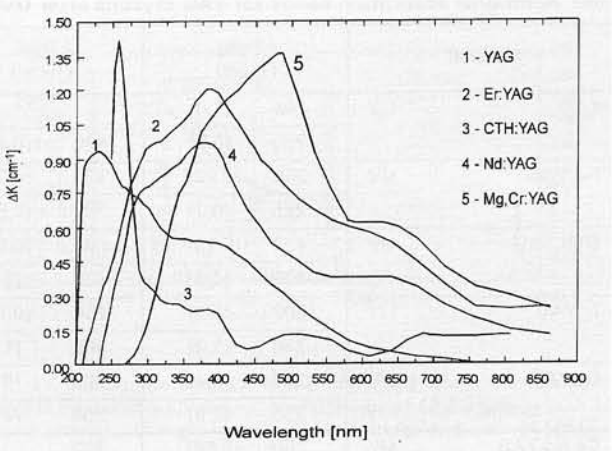


Fig. 3 Additional absorption bands for X:YAG crystals after their excitation with $\gamma$ quanta of 1.25 MeV energy and dose of $10^5$ Gy; X=Er, Cr, Tm, Ho, Nd, Mg

of 15 s between pulses. All the samples were investigated in the same conditions (immediately after excitation). Next, the samples have been excited with $\gamma$ radiation of $5 \times 10^4$ Gy dose emitted by $^{60}$Co source.

In order to determine the absorption coefficient in dependence on wavelength,transmissions of the samples were measured using the following spectrophotometers:

- LAMBDA-2 (Perkin-Elmer) in the spectral range of 200÷1100 nm,
- ACTA VII (Beckman) in the range of 1100÷1400 nm,
- Fourier spectrophotometer FTIR 1725 (Perkin-Elmer) in the range of 1.4÷25 mm. Dispersion of the absorption coefficients was calculated from transmission measurements considering multiple reflections inside the samples.

Displacement of short-wave edge of absorption was not found in any of the investigated materials, but there were found changes of the absorption coefficients near the edge, appearing after UV and $\gamma$ excitation inside the range of 200÷600 nm. Fig. 1 presents AA bands ($\Delta K$) of investigated crystals after UV excitation. It can be seen that among YAG crystals with different dopants Ce:YAG, Pr:YAG, Ce,Nd:YAG ($\Delta K \approx 1$ cm$^{-1}$) show the greatest sensitivity to UV radiation. Nd:YAG, CTH:YAG and Er:YAG are crystals with a weak sensitivity to UV radiation ($\Delta K \approx 0.2$ cm$^{-1}$). It is noticeable that Nd dopant reduces the UV sensitivity of Ce:YAG crystal. Fig. 2 completes the picture for CTH:YAG crystal in comparison with Nd:YAG and pure YAG crystals. The UV sensitivity of CTH:YAG crystal is also weak ($\Delta K \approx 0.2$ cm$^{-1}$).

Fig. 3 presents AA bands for above mentioned crystals after $\gamma$ excitation with dose of $5 \times 10^4$ Gy. As it can be seen, CTH:YAG crystal has weak g sensitivity while Er:YAG crystal is highly sensitive to $\gamma$ radiation. Fig. 4 completes the information for other investigated crystals.

The appearance of AA bands for both UV and $\gamma$ radiations depends, in specific manner, on growth conditions of the crystals (colour centers formed after excitation originate mainly for overcharged growth defects). In Figs 5÷6 there are compared AA bands after UV and g excitations for crystals made in the ITME, examined by us and Prof. Matkowski's group. It can be seen a good qualitative equivalence of the obtained results and only small quantitative variations (displacement of absorption maximum for YAG crystal in Fig. 5, increase of intensity of the absorption maksimum for Nd:YAG after $\gamma$ excitation in comparison with UV excitation in Fig. 6).

In the Table information about absorption maxima for all investigated crystals are presented. Bold-faced print denotes additional maxima appearing after $\gamma$ excitation.

In Figs. 7÷8 the AA bands for Ce:YAG and Ce,Nd:YAG crystals are presented. It can be seen, that Ce:YAG absorption bands have their maxima at 340 and 460 nm. Figs. 9÷11 show absorption bands and overlapping AA bands ($\Delta K$) for CTH:YAG, Nd:YAG and Er:YAG crystals. For CTH:YAG crystal

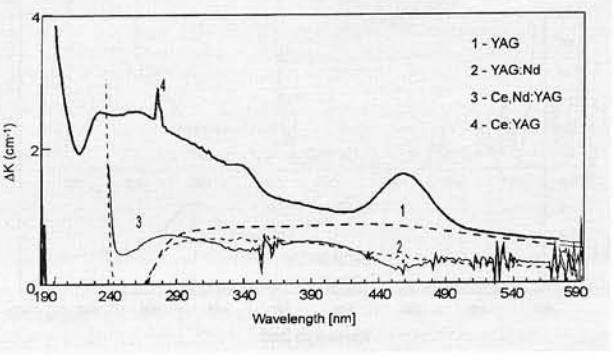


Fig. 4. Additional absorption bands after g excitation of X:YAG crystals; X=Ce, Nd, both Ce and Nd

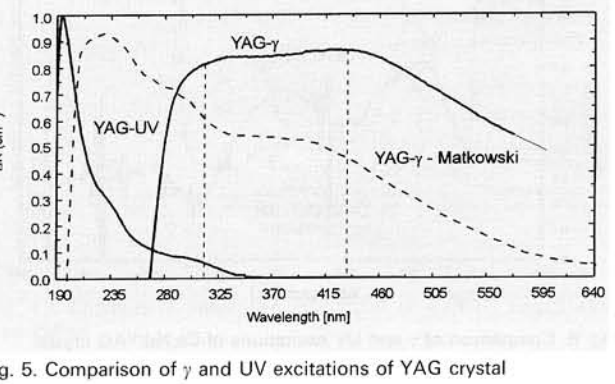


Fig. 5. Comparison of $\gamma$ and UV excitations of YAG crystal

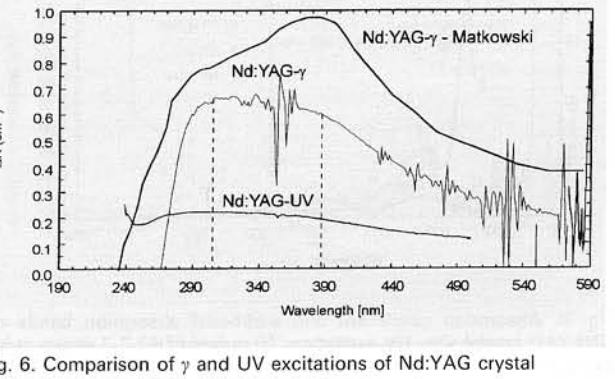


Fig. 6. Comparison of $\gamma$ and UV excitations of Nd:YAG crystal

Table. **Additional absorption bands for YAG crystals after UV and $\gamma$ excitation**

| Material | | $\lambda$ [nm] (1/cm) | $\lambda$ [nm] (1/cm) | $\lambda$ [nm] (1/cm) | $\lambda$ [nm] (1/cm) | $\lambda$ [nm] (1/cm) |
|---|---|---|---|---|---|---|
| YAG | UV | 194 (1.0) | | | | |
| | $\gamma$ | 290 (0.8) | 440 (0.85) | | | |
| Nd:YAG | UV | 285 (0.22) | 320 (0.21) | | | |
| | $\gamma$ | 285 (0.7) | 320 (0.67) | | | |
| CTH:YAG | UV | 430 (0.13) | 600 (0.05) | | | |
| | $\gamma$ | **400 (4.5)** | 430 (3.5) | **485 (3.0)** | 600 (2.0) | |
| Er:YAG | UV | 202 (0.4) | 250 (0.15) | | | |
| | $\gamma$ | 250 (1.0) | **350 (1.2)** | | | |
| Ce:YAG | UV | 235 (0.4) | 260 (0.8) | 310 (0.35) | 390 (0.2) | 500 (0.1) |
| | $\gamma$ | 235 (2.5) | 260 (2.5) | **340 (1.75)** | **460 (1.6)** | |
| Ce,Nd:YAG | UV | 260 (0.62) | 320 (0.3) | 385 (0.27) | 495 (0.18) | |
| | $\gamma$ | **280 (0.68)** | 320 (0.6) | 385 (0.63) | 495 (0.38) | |
| Pr:YAG | UV | 210 (0.5) | 255 (0.9) | 310 (0.6) | 390 (0.4) | |

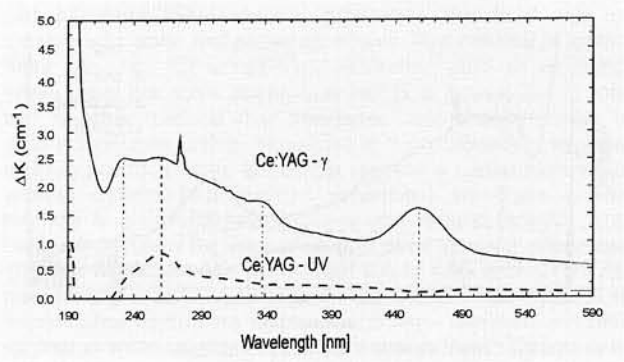


Fig. 7. Comparison of $\gamma$ and UV excitations of Ce:YAG crystal

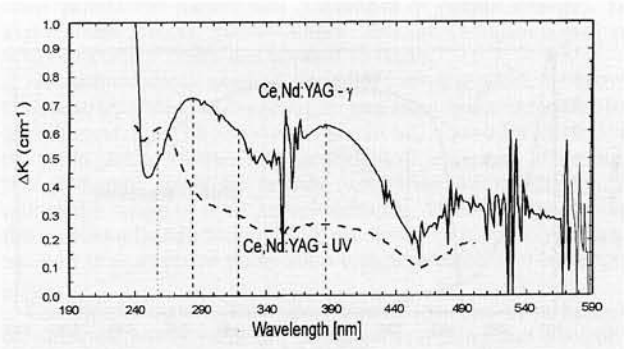


Fig. 8. Comparison of $\gamma$ and UV excitations of Ce,Nd:YAG crystal

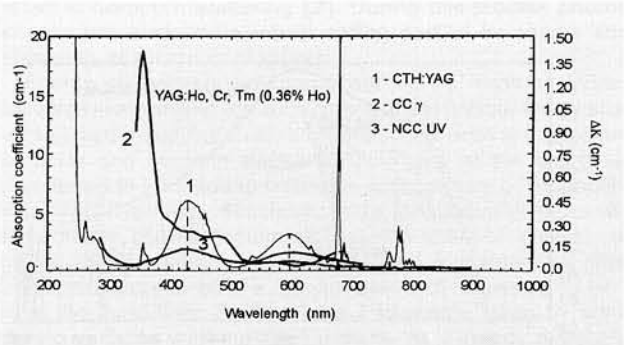


Fig. 9. Absorption coefficient and additional absorption bands of CTH:YAG crystal after UV excitation: 10 pulses of 42.2 J energy with time interval of 15 s and $\gamma$ quanta of 1.25 MeV energy and dose of $10^5$ Gy

AA bands are noticed inside the Cr pumping bands at 430 and 600 nm, both for UV and $\gamma$ excitation. Moreover, there occur additional AA bands for $\gamma$ excitation with their maxima at 400 and 485 nm.

For Nd:YAG crystals we have the similar situation for both types of excitations. Only a change of relative intensity of AA bands takes place. For CTH:YAG crystal the greater $\gamma$ than UV sensitivity is noticeable.

Figs. 12÷14 show that Nd dopant reduces $\gamma$ sensitivity of Ce:YAG and Ce,Nd:YAG crystals.

## 3. Results of lasing investigations

Investigations of free-running laser emission were carried out, using plane-parallel laser resonator with length of 24 cm. The transmissions of output mirrors were equal to 30% for Er:YAG and 20% for CTH:YAG. The laser head consisted of a single, linear xenon flashlamp with diameter of 4 mm and a gold-covered brass reflector. The duration of flashlamp pulse was equal to 250÷300 $\mu$s and the power supply was adjusted within the range of 7 to 300 J. The emitted laser energy was measured by means of Universal Radiometer Rm 6600 (Laser Precision) with RJP-735 probe. The lamp pulses were observed simultaneously on the Tektronix oscilloscope coupled with a high-sensitive Si photodetector.

To define changes of lasing features, Er- and Ho-doped YAG rods have been excited by the same source of $\gamma$ radiation with dose of $10^5$ Gy. The influence of the annealing of the above rods on their laser features was also examined at medium and high temperatures (near melting point). Figs. 15÷18 show the results.

For one of the CTH:YAG crystals it can be noticed that after $\gamma$ excitation (without earlier annealing) the output laser energy increased four times (Fig. 17). The value of threshold of laser emission stayed the same. Another CTH:YAG rod (Fig. 16) significantly improved its generation characteristic (large increase in differential efficiency, decrease in emission threshold) after annealing at high temperature (about 1500°C). Excitation of the laser rod with $\gamma$ radiation gave unstable decrease of laser output energy. After every next pulse (with time intervals of 1 min) laser tended to return to previous generation characteristic (Fig. 15). Annealing this rod at mediumtemperature (about 400°C) improved laser characteristic, but not so significantly as for high temperature annealing.

It results from Fig. 18 that excitation of Er:YAG crystal with $\gamma$ radiation before annealing the laser rod at high temperature, gives twice as large increase of the laser output energy. This change is reversible after annealing the rod at 400°C. The value of threshold of laser emission stays the same.

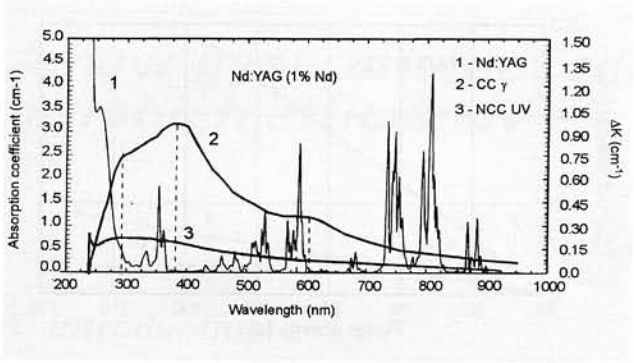


Fig. 10. Absorption coefficient and additional absorption bands of Nd:YAG crystal after UV excitation: 10 pulses of 42.2 J energy with 15 s time interval and g quanta of 1.25 MeV energy and dose of $10^5$ Gy

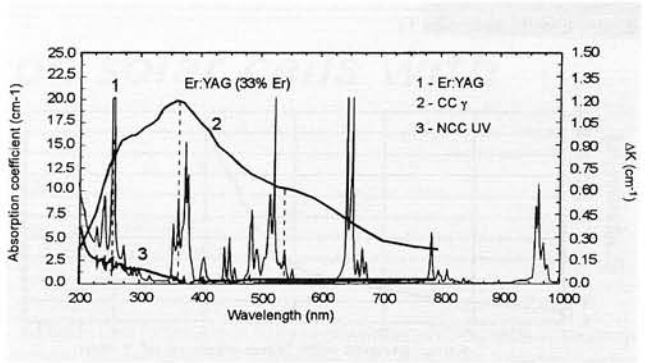


Fig. 11. Absorption coefficient and additional absorption bands of Er:YAG crystal after UV excitation: 10 pulses of 42.2 J energy with 15 s time interval and $\gamma$ quanta of 1.25 MeV energy and dose of $10^5$ Gy

## 4. Conclusions

Under a pulse action of pump lamp it takes place a deterioration of lasing characteristics for lasers from YAG crystals. It is caused by creation of nonstable, short-living at room temperature, colour centers in active elements. Light absorption proceeded by these centers leads to the increase in resonator losses by many percent.

Nonstable colour centers are connected with defects and dopants that have shallow energy levels inside energy gap of the crystals, and therefore electron excitations (electrons, holes, excitons and polarons) are localized there [2]. An excitation of these crystals with ionizing radiation leads to greater feature deterioration, because formed defects increase the quantity of nonstable colour centers. Moreover, there are formed stable colour centers whose absorption increases passive losses in a laser resonator and decreases laser efficiency.

However, there exist materials, including CTH:YAG and Er:YAG crystals, in which AA bands arises inside the pumping bands. An excitation of these materials with $\gamma$ quanta improves their laser features, such as differential efficiency. It showed be said that these materials became strongly defected after their growth process. Moreover, the values of emission thresholds for these materials are very large ($80 \div 100$ J). It is obvious that crystals must not be annealed at high temperatures before excitation, otherwise a deterioration of lasing features takes place. A change of lasing features of the crystals after $\gamma$ excitation reverses after annealing them at the temperature of 400°C by at least 3 hours.

The excitation with $\gamma$ quanta can be an usefullness method for laser feature improving of many crystals, e.g. CTH:YAG, Er:YAG and Nd:YAG crystals [3].

In conclusion: Nd ion decreases UV sensitivity, Cr ion improves lasing characteristics of YAG lasers (also after exciting with $\gamma$ quanta), Pr ion increases UV sensitivity, Ce ion increases UV and $\gamma$ sensitivities (dependently on the concentration [2]) and Er increases $\gamma$ sensitivity of YAG crystals.

It is known that colouring processes of YAG crystals depends, to some extent, on other impurities, e.g. Fe, Ni, Co, W, Mo and Li [2].

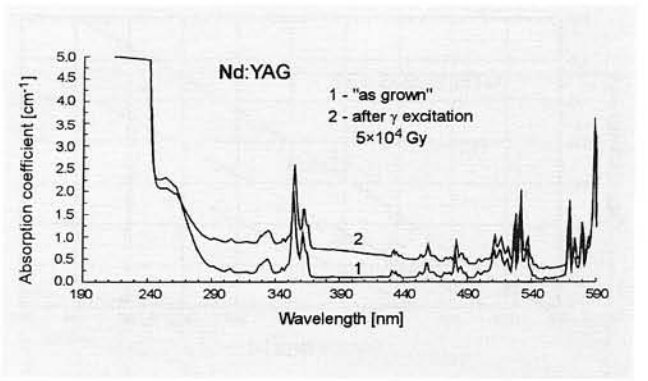


Fig. 12. Changes of absorption coefficient of Nd:YAG crystal after $\gamma$ excitation

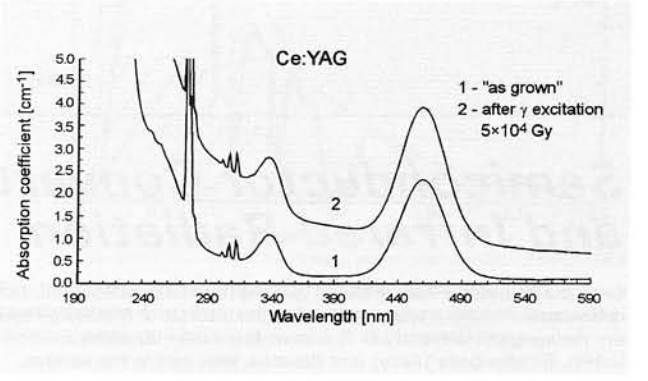


Fig. 13. Changes of absorption coefficient of Ce:YAG crystal after $\gamma$ excitation

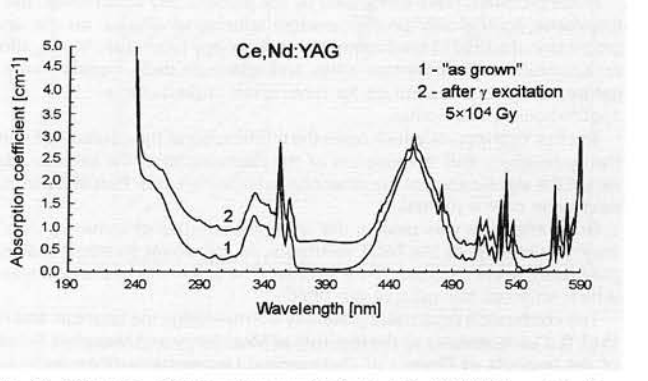


Fig. 14. Changes of absorption coefficient of Ce,Nd:YAG crystal after $\gamma$ excitation ▶

## References


1. *S. Kaczmarek, K. Kopczyński, Z. Mierczyk, A.O. Matkowski, D.J. Sugak, Z. Frukacz*: Influence of $\gamma$-Radiation on Lasing Properties of CTH:YAG and Er:YAG Crystals. Proc. of 4th Conf. on Crystal Growth, Kraksw, 23-24.05.1995.
2. *A.O. Matkowski, D.J. Sugak, S.B. Ubizski, O.I. Shpotyuk, E.A. Czarny, N.M. Vakiw, W.A. Mokrzycki*: Influence of ionizing radiation on electronic technique materials. Swit, Lwiw 1994 (in Russian).
3. *M.R. Bedilov, H.B. Beysembayeva, M.S. Sabitov*: Low-dose irradiation of the lasers on the base of ruby and YAG:$Nd^{3+}$ crystals. Kvantovaya Elektronika, **21** (1994) pp. 1145-1147 (in Russian).

► continued from page 77

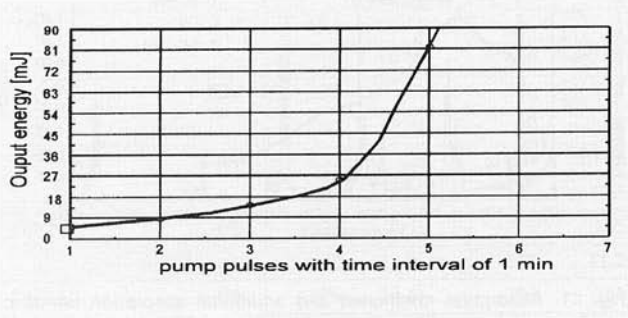


Fig. 15. CTH:YAG G-32 rod after $\gamma$ excitation. Change of output energy after next pump pulse of 135.2 J energy

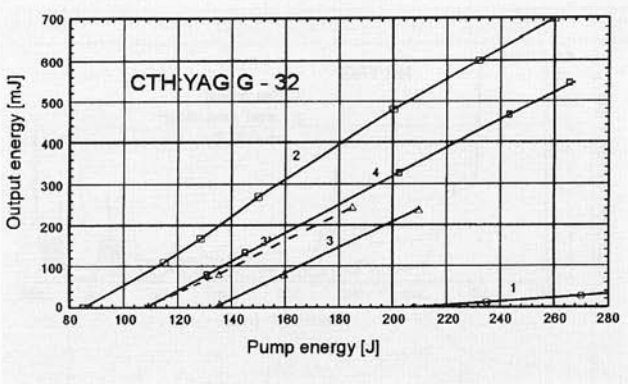


Fig. 16. Change of output energy of CTH:YAG rod after annealing at temperature 1500°C and $\gamma$ excitation: *1* – before annealing, *2* – after annealing in air atmosphere at 1500°C, *3* – and several pulse of 135.2 J energy, *3* – after $\gamma$ excitation ($10^5$ Gy), *4* – after annealing in air by 8 hours at 400°C

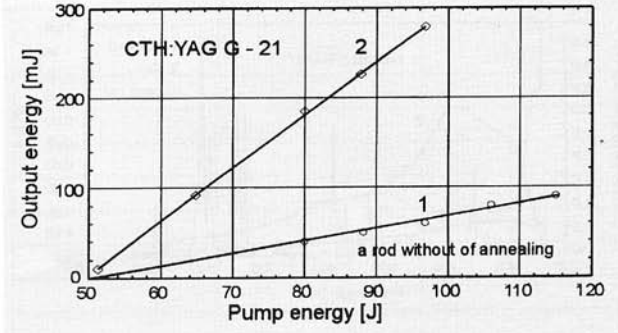


Fig. 17. Change of output energy of CTH:YAG rod without annealing: *1* – CTH:YAG, *2* – CTH:YAG ater 80 days from $\gamma$ excitation and many pulses of the laser

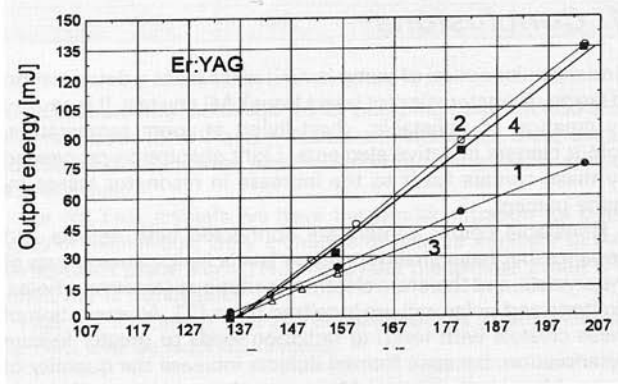


Fig. 18. Change of output energy of Er:YAG laser after $\gamma$ excitation. Influence of the annealing at medium temperatures: *1* – before g excitation, *2* – after $\gamma$ excitation with dose of $10^5$ Gy, *3* – after annealing in air by 8 hours at 400°C, *4* – after $\gamma$ excitation with dose of $5 \cdot 10^4$ Gy